AD-A154 553 THE SOUND FIELD OF A MOVING LASER-INDUCED ACOUSTIC ARRAY (THEORY)(U) TEXAS UNIV AT AUSTIN APPLIED RESEARCH LABS Y H BERTHELOT ET AL. 04 DEC 84 ARL-TR-84-21 1/1

UNCLASSIFIED N00014-82-K-0425 F/G 20/1 NL

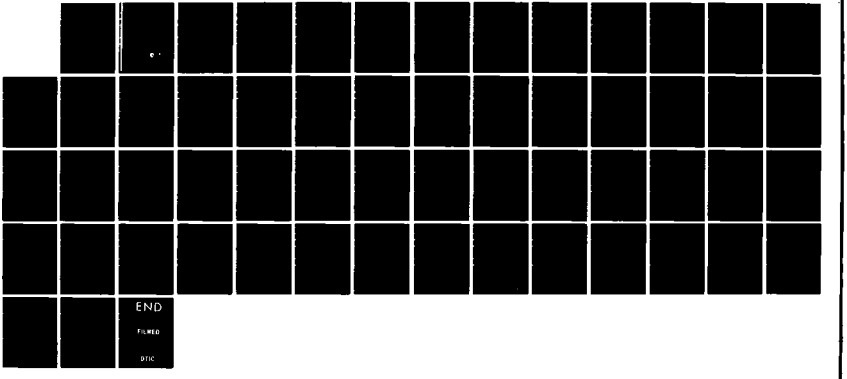

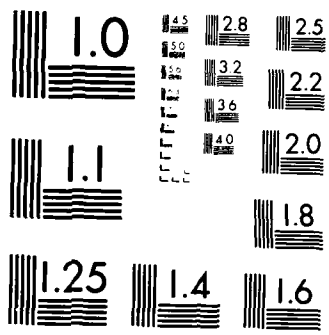

ARL-TR-84-21

Copy No. 4

THE SOUND FIELD OF A MOVING LASER-INDUCED ACOUSTIC ARRAY (THEORY)

Yves H. Berthelot
Ilene J. Busch-Vishniac

APPLIED RESEARCH LABORATORIES
THE UNIVERSITY OF TEXAS AT AUSTIN
POST OFFICE BOX 8029, AUSTIN, TEXAS 78713-8029

4 December 1984

Technical Report

Prepared for:

OFFICE OF NAVAL RESEARCH
DEPARTMENT OF THE NAVY
ARLINGTON, VA 22217

UNCLASSIFIED

SECURITY CLASSIFICATION OF THIS PAGE *(When Data Entered)*

REPORT DOCUMENTATION PAGE		READ INSTRUCTIONS BEFORE COMPLETING FORM
1. REPORT NUMBER	2. GOVT ACCESSION NO.	3. RECIPIENT'S CATALOG NUMBER
4. TITLE *(and Subtitle)* THE SOUND FIELD OF A MOVING LASER-INDUCED ACOUSTIC ARRAY (THEORY)		5. TYPE OF REPORT & PERIOD COVERED technical report 6. PERFORMING ORG. REPORT NUMBER ARL-TR-84-21
7. AUTHOR*(s)* Yves H. Berthelot Ilene J. Busch-Vishniac		8. CONTRACT OR GRANT NUMBER*(s)* N00014-82-K-0425
9. PERFORMING ORGANIZATION NAME AND ADDRESS Applied Research Laboratories The University of Texas at Austin Austin, Texas 78713-8029		10. PROGRAM ELEMENT, PROJECT, TASK AREA & WORK UNIT NUMBERS
11. CONTROLLING OFFICE NAME AND ADDRESS Office of Naval Research Department of the Navy Arlington, Virginia 22217		12. REPORT DATE 4 December 1984 13. NUMBER OF PAGES 52
14. MONITORING AGENCY NAME & ADDRESS*(if different from Controlling Office)*		15. SECURITY CLASS. *(of this report)* UNCLASSIFIED 15a. DECLASSIFICATION/DOWNGRADING SCHEDULE

16. DISTRIBUTION STATEMENT *(of this Report)*

Approved for public release; distribution unlimited.

17. DISTRIBUTION STATEMENT *(of the abstract entered in Block 20, if different from Report)*

18. SUPPLEMENTARY NOTES

19. KEY WORDS *(Continue on reverse side if necessary and identify by block number)*

thermoacoustic array
optoacoustic antenna
impulse response
step response
convolution
exponential shading

20. ABSTRACT *(Continue on reverse side if necessary and identify by block number)*

This report describes the theoretical investigation of the sound field radiated by a moving laser source. When an intensity modulated laser beam illuminates a column of water, it produces a highly directive thermoacoustic array (or opto-acoustic antenna). This report discusses a time domain approach for predicting the pressure field radiated by a moving (subsonic, transonic, or supersonic) thermoacoustic array.

The theory is based on a convolution type summation between the impulse response of the thermoacoustic array and the laser pulse intensity. The theoretical

DD FORM 1 JAN 73 1473 EDITION OF 1 NOV 65 IS OBSOLETE

UNCLASSIFIED

SECURITY CLASSIFICATION OF THIS PAGE*(When Data Entered)*

20. (cont'd)

model is for both nearfield and farfield radiation and for any Mach number of the source.
Numerical results are in very good agreement with a previous study[9] limited to some special cases.
This research is part of Yves Berthelot's work for the degree of Ph.D. under the supervision of Ilene J. Busch-Vishniac.

TABLE OF CONTENTS

LIST OF FIGURES

I. INTRODUCTION

The generation of sound by a light source was suggested more than one hundred years ago by Alexander Graham Bell.[1] It has received more attention recently because of new developments in high power lasers, which make this acoustic generation mechanism more suitable for practical applications.

Westervelt and Larson have shown[2,3] that very directive sound beams of low frequency can be achieved with a thermoacoustic array (or optoacoustic antenna). A thermoacoustic array is an acoustic line source obtained by shining a laser into a medium. Optical absorption in the medium induces an exponential tapering of the line source along the axis of penetration of the laser beam. The principle of operation of these arrays is that amplitude modulation of the intensity of the laser beam, directed toward the absorptive medium (usually water), induces a periodic heating of the medium and therefore a fluctuation of density. This in turn generates an acoustic wave in the medium. The acoustic frequency is thus equal to the modulation frequency of the laser intensity.

The first experimental verifications of thermoacoustic radiation were made by Muir et al.[4,5] and Culbertson[6] and, as expected, the efficiency of the conversion of electromagnetic energy into acoustic energy was extremely low. However, recent studies by Bunkin et al.[7,8] have shown that the amplitude of the acoustic signal can be increased by moving the laser beam at high velocities through the water. High speed motion of the beam can easily be achieved using a rotating mirror; therefore a mechanical transducer moving in the medium is not required.

This report describes a simple time domain method which can be used to compute the pressure waveform radiated by a moving thermoacoustic array (MTA). In Section II, we shall derive an expression for the acoustic response observed in a medium when the optoacoustic source is an ideal impulse. In this case, the acoustic response will be called the impulse

response of a thermoacoustic array (TA). It is assumed that the light source is in the form of a narrow beam striking the medium at normal incidence. In Section III, the impulse response of a TA will be used to compute the pressure waveform radiated by a source moving at any velocity through an optically absorbing medium.

There are three main reasons for choosing the impulse response approach rather than a frequency response approach: (1) it gives analytical results valid in both the nearfield and farfield of the source, (2) the theory does not break down for transonic motion of the source, and (3) time information is presented without need for a transform.

In Section IV the time domain method is compared to a previous theory developed by Lyamshev and Sedov[9] for the special case of farfield radiation with analytical predictions based on the impulse response approach. It will be shown that the two theories are essentially in agreement.

The main conclusions of this study will be summarized in the last section.

II. IMPULSE RESPONSE OF A THERMOACOUSTIC ARRAY

In this section an analytical expression is derived for the impulse response of a thermoacoustic array. The first step is to solve the wave equation and derive an expression in integral form for the acoustic pressure in terms of the optical intensity of the source. The impulse response is then obtained by letting the source function be replaced by a delta function.

A. Analytical Approach

The wave equation for a viscous medium containing heat sources is derived in Appendix A. For an inviscid, non heat conducting fluid, the linearized wave equation takes the form

$$\nabla^2 p - \frac{1}{c^2} \frac{\partial^2 p}{\partial t^2} = - \frac{\beta}{c_p} \frac{\partial q}{\partial t} \quad , \tag{1}$$

where

p is the acoustic pressure,

c is the small signal sound speed,

$q = - \nabla \cdot I(x,y,z,t)$ is energy per unit volume and per unit time added to the medium,

I is the laser intensity,

β is the logarithmic coefficient of thermal expansion of the medium, and

c_p is the specific heat of the medium at constant pressure.

The solution to Eq. (1) for a pressure release air-water interface is obtained by integrating the Green's function of the problem over the source region.

$$p = \frac{\beta}{4\pi c_p} \iiint_{V_{water}} \frac{1}{r} \frac{\partial q\left(t - \frac{r}{c}\,;\, r\right)}{\partial t} dV$$

$$- \frac{\beta}{4\pi c_p} \iiint_{V_{air}} \frac{1}{r'} \frac{\partial q\left(t - \frac{r'}{c}\,;\, r'\right)}{\partial t} dV \quad . \tag{2}$$

Here r and r' are distances from the source to the receiver and are shown in Fig. 1.

Equation (2) gives the acoustic pressure p observed at the receiver at any point in the field. The first integral in Eq. (2) represents the contribution of the thermoacoustic source located in the water, and therefore the volume of integration is the volume V_{water} of the column of water being irradiated by the laser beam. The second term in Eq. (2) represents the effect of the image sources located above the interface, and therefore the volume of integration is V_{air}, the mirror image of V_{water} (see Fig. 1.). The minus sign is due to the compliant nature of the interface. These two contributions are not identical because the time lags r/c and r'/c are different for the volumes of integration. For a uniform intensity distribution across the beam, the energy q reduces to

$$q = - \frac{\partial}{\partial z} \left[A\, I(t)\, e^{-\alpha z}\right] \quad , \tag{3}$$

where A is the optical transmissivity from air to water, and $e^{-\alpha z}$ is the exponential tapering with depth associated with the absorption of light in water.

Assuming that the beam diameter is always very small compared to the characteristic wavelength λ of the acoustic radiation, we rewrite Eq. (2) in the following form:

$$p = \frac{\beta S}{4\pi c_p} \int_z \frac{1}{r} \frac{\partial q\left(t - \frac{r}{c}\,;\, r\right)}{\partial t} dz \; - \frac{\beta S}{4\pi c_p} \int_z \frac{1}{r'} \frac{\partial q\left(t - \frac{r'}{c}\,;\, r'\right)}{\partial t} dz \,, \tag{4}$$

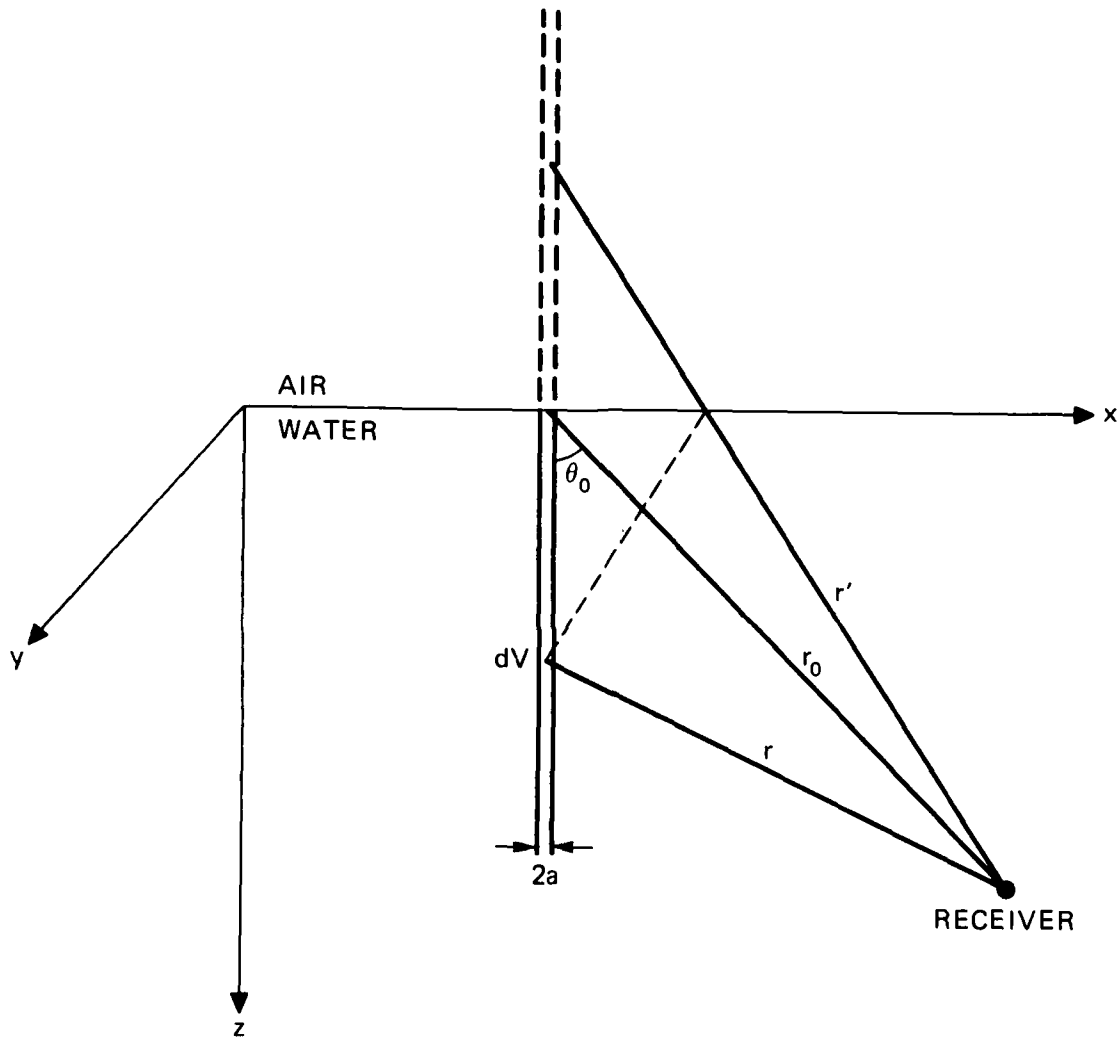

FIGURE 1
GEOMETRY OF THE ARRAY

ARL:UT
AS-84-781
YHB - GA
9 - 5 - 84

where $S=\pi a^2$ is the beam cross section. For a laser pulse whose intensity is modulated at frequency f, the characteristic acoustic wavelength is $\lambda = c/f$; for an unmodulated laser pulse, $\lambda = c\tau_p$, where τ_p is the pulse duration.

Combining Eqs. (3) and (4), we obtain a general expression for the acoustic pressure in terms of the laser intensity:

$$p = \frac{A\beta S\alpha}{4\pi c_p} \int_z \frac{e^{-\alpha z}}{r} \frac{\partial I\left(t - \frac{r}{c}\right)}{\partial t} dz - \frac{A\beta S\alpha}{4\pi c_p} \int_z \frac{e^{-\alpha z}}{r'} \frac{\partial I\left(t - \frac{r'}{c}\right)}{\partial t} dz. \quad (5)$$

Equation (1) shows that the optoacoustic source strength (forcing function) is proportional to the time derivative of the laser intensity. It is therefore convenient to define the impulse response h(t) by

$$p(t) = h(t) * \frac{\partial I}{\partial t} \quad , \quad (6)$$

where the asterisk denotes convolution. The function h(t) is therefore the acoustic response to an impulse dI/dt. Consequently, h(t) can be regarded as either the optoacoustic impulse response or the light step response. From Eq. (5) we find

$$h(t) = \frac{A\beta S\alpha}{4\pi c_p} \int_z \frac{e^{-\alpha z}}{r} \delta\left(t - \frac{r}{c}\right) dz - \text{mirror image} \quad . \quad (7)$$

Shifting the integration variable from z to r, we rewrite Eq. (7) as

$$h(t) = \frac{A\beta S\alpha c}{4\pi c_p} \int_z \frac{e^{-\alpha z(r)}}{r} \delta(r-ct) \left(\frac{dz}{dr}\right) dr - \text{mirror image} \quad . \quad (8)$$

Equation (8) provides a means for evaluating the impulse response of a thermoacoustic array once the relationship between the depth z and radius of observation r or r' is known. Assuming that the laser beam strikes the water at normal incidence, the array may be divided into four regions. These are indicated in Fig. 2. For each region the relationship between z and r or r' is given below.

-region 1 (mirror image):

$$-\infty < z \leq 0 \quad ; \quad r_0 \leq r' < \infty$$

$$z = -r_0 \cos\theta_0 + \sqrt{r'^2 - r_0^2 \sin^2\theta_0}$$

$$\frac{dz}{dr'} = \frac{r'}{\sqrt{r'^2 - r_0^2 \sin^2\theta_0}}$$

-region 2:

$$0 \leq z \leq r_0 \cos\theta_0 \quad ; \quad r_0 \sin\theta_0 \leq r \leq r_0$$

$$z = -r_0 \cos\theta_0 + \sqrt{r^2 - r_0^2 \sin^2\theta_0}$$

$$\frac{dz}{dr} = \frac{-r}{\sqrt{r^2 - r_0^2 \sin^2\theta_0}}$$

-region 3:

$$r_0 \cos\theta_0 \leq z \leq 2r_0 \cos\theta_0 \; ; \; r_0 \sin\theta_0 \leq r \leq r_0$$

$$z = r_0 \cos\theta_0 + \sqrt{r^2 - r_0^2 \sin^2\theta_0}$$

$$\frac{dz}{dr} = \frac{r}{\sqrt{r^2 - r_0^2 \sin^2\theta_0}}$$

-region 4:

$$z \geq 2r_0 \cos\theta_0 \quad ; \quad r_0 \leq r < \infty$$

time delay $i \cdot \Delta t$ taken by the source to travel from the origin (t=0) to the ith position. This gives the total acoustic pressure $p_T(t)$ radiated by the thermoacoustic array during its motion:

$$p_T(t) = \sum_{i=0}^{N} p_i(t-i \cdot \Delta t)\Delta t \quad . \tag{19}$$

Combining Eqs. (18) and (19) finally gives

$$p_T(t) = \sum_{i=0}^{N} I'(i \cdot \Delta t)\, h_i(t-i \cdot \Delta t)\Delta t \quad . \tag{20}$$

Equation (20) shows that the total pressure received at the observation point is a convolution type summation in the time domain, between the "unsteady" (changing shape with time) impulse response $h_i(t)$ and the optoacoustic source strength dI/dt. Note that in the case of a stationary array, the shape of impulse response remains constant and the *numerical program performs* a true convolution between the impulse response and the optoacoustic source strength.

This time domain approach is perfectly suitable for a numerical computation, and a program to perform the computation has been written on the ARL:UT CYBER computer.

B. Farfield Criterion

The farfield criterion has been a source of confusion in the literature on thermoacoustic arrays. It seems necessary to state clearly the difference between the geometric farfield (Fresnel approximation), the acoustic farfield, and a farfield criterion based upon the source dimensions (Fraunhofer approximation), for both stationary and moving sources, with or without intensity modulation of the laser pulse. The geometric farfield depends upon the dimension(s) of the source relative to the distance of observation. The acoustic farfield depends upon the distance of observation relative to a typical acoustic wavelength. The

The second step is to compute for each of these positions the elementary acoustic pressure $p_i(t)$ radiated by the array when it was at the position shown on the ith picture, that is to say, after a time delay $i \cdot \Delta t$. The laser source intensity at that instant is simply $I(i \cdot \Delta t)$ and the impulse response $h_i(t)$ can be evaluated from Eqs. (10)-(14). However, it is very important to realize that the impulse response is a function of the position of the array because the distance r_0 and the angle θ_0 between the source and the receiver are time dependent in the case of a moving source. Let us denote by r_i and θ_i the values of r_0 and θ_0 shown on the ith picture corresponding to time $i \cdot \Delta t$ after the beginning of the motion of the source. It can very easily be shown that

$$r_i = \sqrt{\hat{r}_0^{\,2} - 2\hat{r}_0 (v.i \cdot \Delta t) \cos\hat{\theta}_0 + (v.i \cdot \Delta t)^2} \qquad (16)$$

and

$$\theta_i = \cos^{-1}\left(\frac{\hat{r}_0 \cos\hat{\theta}_0}{r_i}\right) \quad , \qquad (17)$$

where $\hat{r}_0$ and $\hat{\theta}_0$ refer to values at the origin of the motion of the source (t=0). The impulse response $h_i(t)$ is therefore given by the set of Eqs. (10)-(14) where the coordinates r_0 and θ_0 have been replaced by r_i and θ_i , using Eqs. (16) and (17).

The elementary acoustic pressure $p_i(t)$ is then computed as follows. Equation (6) shows that the optoacoustic source strength is proportional to the time derivative of the laser intensity. Therefore during the ith picture, the optoacoustic strength is $\left.\frac{dI}{dt}\right|_{t=i \cdot \Delta t}$ or, in a shorthand notation, $I'(i \cdot \Delta t)$. The ith picture therefore shows an array excited by an impulse of strength $I'(i \cdot \Delta t)$, and then $p_i(t)$ is given by

$$p_i(t) = I'(i \cdot \Delta t) h_i(t) \quad . \qquad (18)$$

The last step is then to add all the elementary acoustic pressures $p_i(t)$ radiated during the motion of the source, taking into account the

III. MOVING THERMOACOUSTIC ARRAY

It has been shown in the previous section that the acoustic impulse response of a thermoacoustic array is described by Eqs. (10)-(14). In this section we seek a solution for the pressure field radiated by a moving thermoacoustic array (MTA) in terms of its impulse response. It is assumed in what follows that the observation point is on the plane of motion of the source.

A. Time Domain Analysis

The pressure radiated by an MTA can be constructed in a three-step procedure. First, the motion of the source can be decomposed in time. As in a movie, a "picture" can be taken at constant time intervals Δt, showing the laser beam at different positions along its path during the laser pulse duration τ_p. Second, for each of these positions (defined by the subscript i) the impulse response $h_i(t)$ and the corresponding elementary pressure response $p_i(t)$ may be computed numerically from Eqs. (10)-(14). Third, the total pressure $p_T(t)$ received at the hydrophone can then be obtained by adding all of the elementary acoustic responses $p_i(t)$ with the suitable time delays corresponding to the motion of the source. Note that this approach is also suitable for a source moving with a nonuniform velocity along its path; however, in the following analysis, it will be assumed for simplicity that the source is moving at a constant velocity v.

The first step in the analysis is a discretization in time and space of the motion of the source so that the problem can be analyzed numerically on a computer. Given that τ_p is the laser pulse duration and Δt the time increment, the motion of the source is represented by N pictures taken every Δt seconds, such that $N = \tau_p / \Delta t$. For a source moving rectilinearly at constant velocity v, $i \cdot \Delta t$ represents the time taken for the array to move from the origin to the position shown on the ith picture.

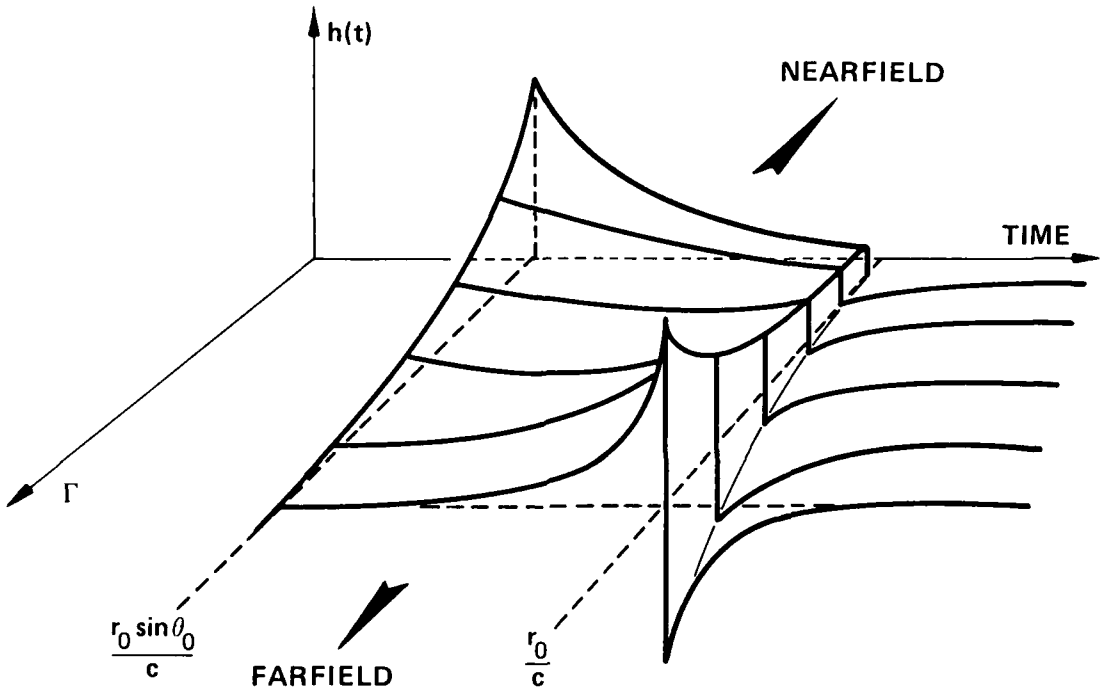

FIGURE 4
IMPULSE RESPONSE AS A FUNCTION OF $\Gamma = \alpha r_0 \cos\theta_0$

ARL:UT
AS-83-1131-V
YHB - GA
10 - 24 - 83
REV 8-21-84

$$\left.\frac{dh}{dt}\right|_{t=t_{min}} = 0 \quad ,$$

with h(t) defined by Eq. (11), leads to $\tanh(\alpha\mu_{min}) = 1/\alpha\mu_{min}$, i.e.,

$$\alpha\mu_{min} \simeq 1.2 \quad ,$$

where

$$\mu_{min} = \sqrt{(ct_{min})^2 - r_o^2 \sin^2\theta_o} \quad .$$

Figure 4 shows the evolution of the impulse response function h(t) in the Γ-t plane.

strongest disturbance is therefore the one which suffers the least spherical spreading loss. Consequently the strongest disturbance is originated by the elementary source on the array which is the closest to the receiver. Since the minimum distance between the source and the receiver is $r_0 \sin\theta_0$, the impulse response h(t) exhibits a peak at time $r_0 \sin\theta_0/c$ and then decreases gradually until $t=r_0/c$.

It is also interesting to note that the first effect (exponential decay in the source strength along the z axis) dominates the second effect (spherical spreading loss) when the observation point is located in the farfield. Reciprocally, the second effect becomes predominant when the observation point is situated in the nearfield. This means that in the farfield most of the acoustic response occurs at $t=r_0/c$, while in the nearfield most of it is expected to occur at $t=r_0 \sin\theta_0/c$. To show this, let us recall that the observation point is said to be in the geometrical farfield when the vertical diffraction loss of the array can be neglected. This will be discussed in more detail in Section III.B. This farfield approximation is in fact equivalent to neglecting the difference in spherical spreading between all the elementary sources of the array. The remaining mechanism determining the shape of the impulse response h(t) is thus, in the geometric farfield, the exponential tapering along the z axis.

Reciprocally, in the nearfield, the difference of path from the elementary sources of the array to the observation point can be quite different from one elementary source to another. The spherical spreading loss associated with this difference of path is, in the nearfield, always more important than the exponential shading along the z axis, and therefore dictates the shape of the impulse response h(t).

This approach may be used to define a geometrical nearfield criterion. When both spherical spreading and exponential shading are of the same importance, the impulse response exhibits two peaks of approximately equal magnitude at time $t=r_0 \sin\theta_0/c$ and $t_0=r_0/c$ (see Fig. 3 for the case $\Gamma = 3$). Thus h(t) passes through a minimum value at a time t_{min}, such that $t_1<t_{min}<t_0$ evaluating

and I_n and K_n are the modified Bessel functions of first and second kind of order n.

B. Discussion

The following section is a detailed analysis of the behavior of the impulse response h(t) when $r_o \sin\theta_o/c < t < r_o/c$, whose aim is to provide some understanding of the nearfield of a thermoacoustic array. The shape of h(t) can change drastically from a monotonically decreasing function with a maximum at $t=r_o\sin\theta_o/c$, to a monotonically increasing function having a maximum at $t=r_o/c$. This curious behavior can be explained by looking at the two different effects determining the shape of the impulse response: the exponential shading $e^{-\alpha z}$ along the axis of the array, which is due to the absorption of light in the medium, and the spherical spreading associated with each wavelet radiated by the thermoacoustic array.

For simplicity let us first assume that the exponential decay along the depth of the TA is much more important than the spherical spreading. Let z_A, z_B, z_C, and z_D be the depths of the elementary sources located at points A, B, C, and D on the array as shown in Fig. 2. It can be shown that, for any positive α,

$$e^{-\alpha z_B} + e^{-\alpha z_C} < e^{-\alpha z_A} + e^{-\alpha z_D} \quad .$$

Therefore the strength of the acoustic disturbance coming from points B and C is always less important than the strength of the one originating at points A and D. Since the latter arrives at the receiving point at time r_o/c, the impulse response h(t) is expected to increase gradually from time $r_o\sin\theta_o/c$ to time r_o/c.

If we assume now that the spherical spreading loss is much more important than the exponential decay of the source strength along the array, all elementary sources have approximatively the same strength. The

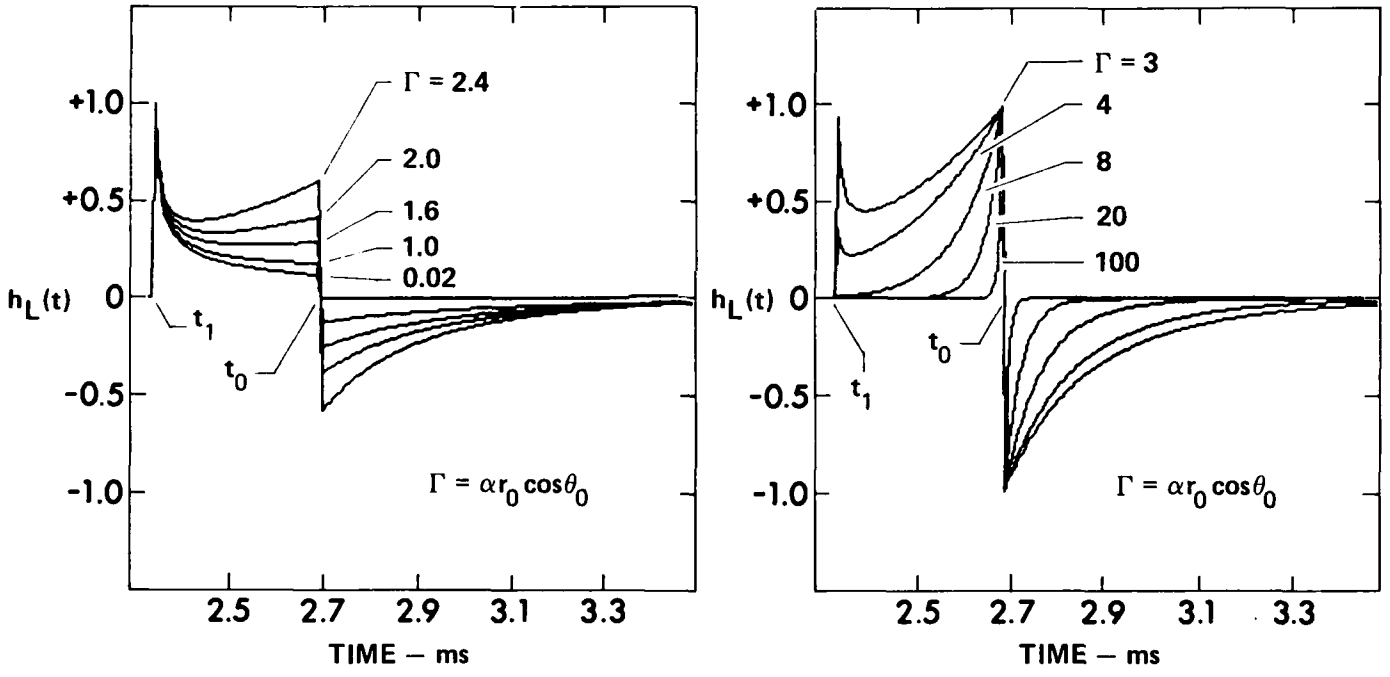

$r_0 = 4$ m $\quad \theta_0 = 60°$

$t_0 = r_0/c \quad t_1 = r_0 \sin\theta_0/c$

FIGURE 3
IMPULSE RESPONSE OF A THERMOACOUSTIC ARRAY

ARL:UT
AS-83-1130-S
YHB-GA
10-24-83

with

$$K = \frac{A \beta S \alpha c}{4 \pi c_p} ,$$

$$t_o = \frac{r_o}{c} ,$$

$$t_1 = \frac{r_o \sin\theta_o}{c} ,$$

$$\Gamma = \alpha r_o \cos\theta_o \quad , \text{ and}$$

$$\mu = c\sqrt{t^2 - t_1^2} \quad .$$

Figure 3 shows how the shape of the impulse response h(t) changes as the nondimensional parameter $\Gamma = \alpha r_o \cos\theta_o$ is varied from 0.02 to 100. (Γ is the ratio of the depth of the receiver to the effective length α^{-1} of the thermoacoustic array.) It is assumed that the laser is shined into fresh water with c = 1486 m/sec.

The impulse response h(t) may also be expressed in terms of modified Bessel functions. The relationship between hyperbolic functions and modified Bessel functions is given in Ref. 10, p. 443. It can easily be shown that

$$h(t) = \begin{cases} 0 & \text{for } t < t_1 \\ K e^{-\Gamma} (r_o \sin\theta_o)^{-1} & \text{for } t = t_1 \\ \sqrt{2\pi}\ K\alpha\ e^{-\Gamma}\ \rho^{-1/2}\ I_{-1/2}(\rho) & \text{for } t_1 < t < t_o \\ K e^{-2\Gamma} (r_o)^{-1} & \text{for } t = t_o \\ -2\sqrt{\frac{2}{\pi}}\ K\alpha\ \sinh(\Gamma)\ \rho^{-1/2}\ K_{1/2}(\rho) & \text{for } t > t_o \end{cases} , \qquad (15)$$

where

$$\rho = \alpha\mu = \alpha\sqrt{(ct)^2 - r_o^2 \sin^2\theta_o}$$

$$h(t) = K \frac{e^{-2\alpha r_o \cos\theta_o}}{r_o} \quad . \tag{13}$$

5. $t > r_o/c$

The disturbances emitted by regions 1 and 4 of the TA will arrive by pairs at the observation point. However, in this case the boundary condition at the air-water interface (pressure release) implies that signals coming from region 1 (mirror image) are inverted. In this time region the only nonzero contribution to the impulse response is given by the last two integrals in Eq. (9). These may be evaluated to yield

$$h(t) = \frac{K}{\sqrt{(ct)^2 - r_o^2 \sin^2\theta_o}} \left\{ \exp\left[-\alpha\left(r_o \cos\theta_o + \sqrt{(ct)^2 - r_o^2 \sin^2\theta_o}\right)\right] \right.$$

$$\left. - \exp\left[-\alpha\left(-r_o \cos\theta_o + \sqrt{(ct)^2 - r_o^2 \sin^2 - \theta_o)}\right)\right]\right\} \quad ,$$

which can be rewritten in simpler form by using the hyperbolic sine,

$$h(t) = \frac{-2K \exp\left[-\alpha\sqrt{(ct)^2 - r_o^2 \sin^2\theta_o}\right]}{\sqrt{(ct)^2 - r_o^2 \sin^2\theta_o}} \sinh(\alpha r_o \cos\theta_o) \quad . \tag{14}$$

The impulse response of a thermoacoustic array as a function of time is therefore given by the set of Eqs. (10)-(14).

$$h(t) = \begin{cases} 0 & \text{for } t < t_1 \quad \text{Eq. (10)} \\ K e^{-\Gamma} (r_o \sin\theta_o)^{-1} & \text{for } t = t_1 \quad \text{Eq. (11)} \\ 2K e^{-\Gamma} \mu^{-1} \cosh(\alpha\mu) & \text{for } t_1 < t < t_o \quad \text{Eq. (12)} \\ K e^{-2\Gamma} (r_o)^{-1} & \text{for } t = t_o \quad \text{Eq. (13)} \\ -2K \mu^{-1} e^{-\alpha\mu} \sinh(\Gamma) & \text{for } t > t_o \quad \text{Eq. (14)} \end{cases}$$

3. $\frac{r_o \sin\theta_o}{c} < t < \frac{r_o}{c}$

By referring to Fig. 2, it is obvious that the first wavelet that will reach the receiver emanates from point E. A short instant later, wavelets coming from points B and C will arrive simultaneously at the receiver. The progression continues with wavelets eventually arriving from points A and D. These are the wavelets received during the interval $r_o \sin\theta_o/c < t < r_o/c$.

The disturbances coming from regions 2 and 3 of the TA, then, will add coherently by pairs at the observation point. The only nonzero contribution to the impulse response is given by the first two integrals in Eq. (9), which may be evaluated to give

$$h(t) = \frac{K}{\sqrt{(ct)^2 - r_o^2 \sin^2\theta_o}} \left\{ \exp\left[-\alpha \left(r_o \cos\theta_o - \sqrt{(ct)^2 - r_o^2 \sin^2\theta_o} \right) \right] + \exp\left[-\alpha' \left(r_o \cos\theta_o + \sqrt{(ct)^2 - r_o^2 \sin^2\theta_o} \right) \right] \right\} .$$

This expression can be simplified by introducing the hyperbolic cosine,

$$h(t) = \frac{2K\, e^{-\alpha r_o \cos\theta_o}}{\sqrt{(ct)^2 - r_o^2 \sin^2\theta_o}} \cosh\left[\alpha \sqrt{(ct)^2 - r_o^2 \sin^2\theta_o} \right] . \qquad (12)$$

4. $t = r_o/c$

There are two points on the array which are located at a distance r_o from the receiver. These two points are denoted A and D on Fig. 2. The impulse response at $t=r_o/c$ is thus the sum of both wavelets coming from points A and D. The pressure release boundary condition at the free surface of the liquid implies that the acoustic contribution from point A is zero. Therefore the impulse response at $t=r_o/c$ is simply given by the wavelet coming from D, that is to say from the point of the array located at a depth $z=2r_o\cos\theta_o$. Equation (7) yields an expression for the impulse at $t=r_o/c$,

$t < r_o \sin\theta_o/c$,
$t = r_o \sin\theta_o/c$,
$r_o \sin\theta_o/c < t < r_o/c$,
$t = r_o/c$, and
$t > r_o/c$.

Using Eq. (9) it is possible to find the impulse response h(t) for the five time regimes.

1. $t < r_o \sin\theta_o/c$

The impulse response reduces to

$$h(t) = 0 \quad , \tag{10}$$

which states that the acoustic emission from the array has not yet had time to arrive at the source. The first disturbance emitted by the TA has to travel a distance $r_o\sin\theta_o$ before reaching the observation point. Therefore the impulse response h(t) is expected to be identically zero for any time $t<r_o\sin\theta_o/c$.

2. $t = r_o \sin\theta_o/c$

Since $r_o\sin\theta_o$ represents the shortest distance between the source and the receiver (see Fig. 2), the particular instant $t=r_o\sin\theta_o/c$ represents the time of arrival of the first wavelet at the receiver. This wavelet was originated at a distance $r_o\sin\theta_o$ from the receiver, that is to say, at a depth $z=r_o\cos\theta_o$ on the array. Consequently, the impulse response is, simply, from Eq. (7),

$$h(t) = \frac{K\, e^{-\alpha r_o \cos\theta_o}}{r_o \sin\theta_o} \quad . \tag{11}$$

$$z = r_o \cos\theta_o + \sqrt{r^2 - r_o^2 \sin^2\theta_o}$$

$$\frac{dz}{dr} = \frac{r}{\sqrt{r^2 - r_o^2 \sin^2\theta_o}}$$

Expanding Eq. (8) in separate integrals over the four regions leads to

$$h(t) = K \int_{r_o}^{r_o \sin\theta_o} \frac{\delta(r-ct)}{r} \exp\left[-\alpha\left(r_o \cos\theta_o - \sqrt{r^2 - r_o^2 \sin^2\theta_o}\right)\right] \frac{-rdr}{\sqrt{r^2 - r_o^2 \sin^2\theta_o}}$$

$$+ K \int_{r_o \sin\theta_o}^{r_o} \frac{\delta(r-ct)}{r} \exp\left[-\alpha\left(r_o \cos\theta_o + \sqrt{r^2 - r_o^2 \sin^2\theta_o}\right)\right] \frac{rdr}{\sqrt{r^2 - r_o^2 \sin^2\theta_o}}$$

$$+ K \int_{r_o}^{\infty} \frac{\delta(r-ct)}{r} \exp\left[-\alpha\left(r_o \cos\theta_o + \sqrt{r^2 - r_o^2 \sin^2\theta_o}\right)\right] \frac{rdr}{\sqrt{r^2 - r_o^2 \sin^2\theta_o}}$$

$$- K \int_{o}^{\infty} \frac{\delta(r-ct)}{r} \exp\left[-\alpha\left(-r_o \cos\theta_o + \sqrt{r^2 - r_o^2 \sin^2\theta_o}\right)\right] \frac{rdr}{\sqrt{r^2 - r_o^2 \sin^2\theta_o}}, \quad (9)$$

where

$$K = \frac{A \beta S \alpha c}{4 \pi c_p} \quad .$$

The four integrals on Eq. (9) represent the contributions to the acoustic pressure from the four array regions defined previously. However, it is more physically meaningful to distinguish the array response by regions in time rather than in space. The limits of integration indicate that the analysis of the impulse response should be divided into five time regimes:

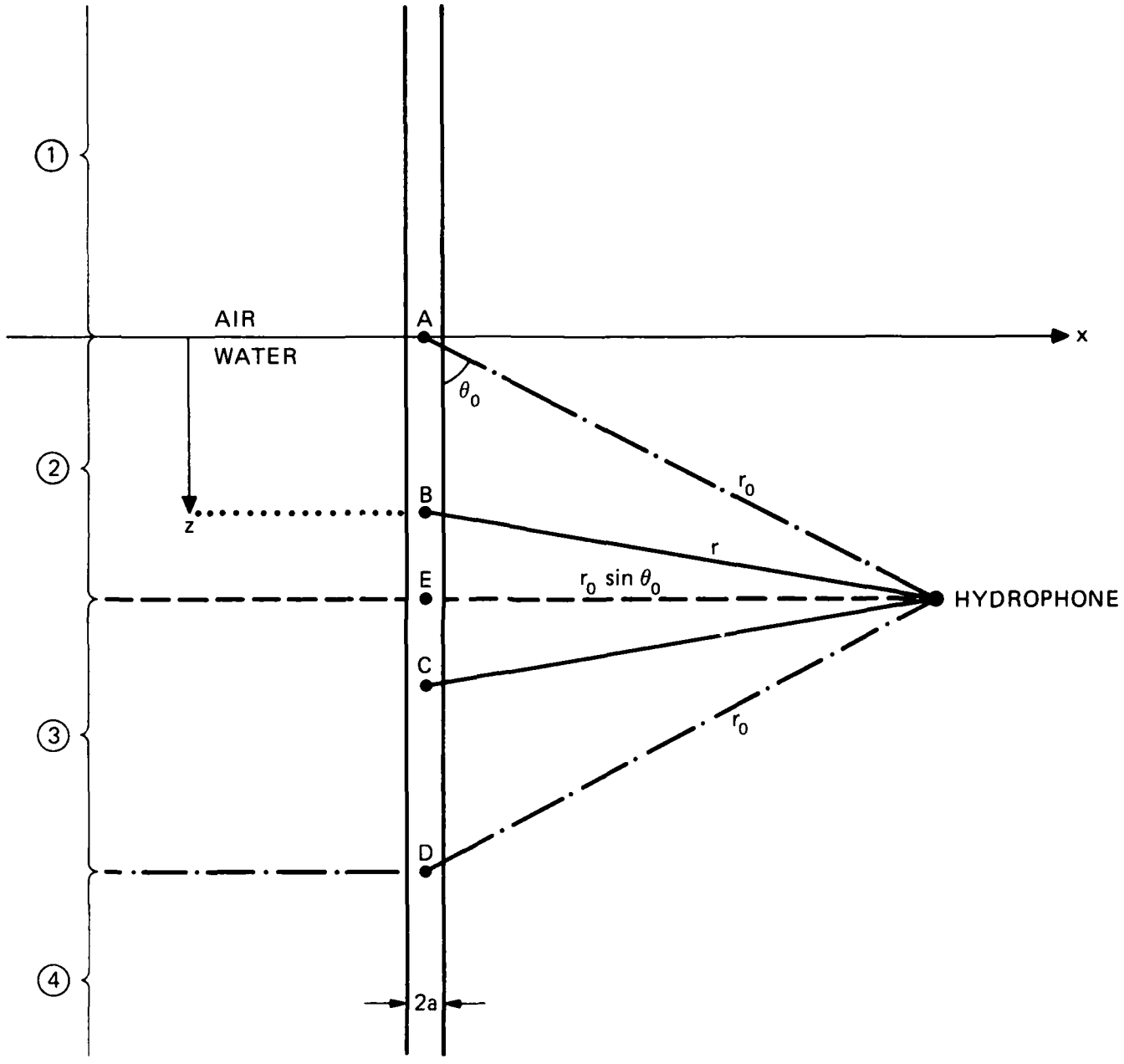

FIGURE 2
GEOMETRY OF THE ARRAY

ARL:UT
AS-84-782
YHB - GA
9 - 5 - 84

source dimensions approximation depends upon the dimensions of the source relative to a typical acoustic wavelength.

1. Geometric Farfield

a. Stationary Source

It can be seen from Fig. 5 that, for an array of effective length $L=\alpha^{-1}$, the radial distances to the receiver from the array depths $z=0$ and $z=L$ are related according to

$$r_L = r_o \left[1 - 2\left(\frac{L}{r_o}\right)\cos\theta_o + \left(\frac{L}{r_o}\right)^2\right]^{1/2} \quad . \tag{21}$$

The Fresnel approximation[11] for the geometric farfield is given by

$$\frac{L}{r_o} << 1 \quad . \tag{22}$$

If this approximation is met, Eq. (21) may be rewritten as

$$r_L \simeq r_o - L\cos\theta_o \quad . \tag{23}$$

We may define a time delay τ_L as

$$\tau_L = \frac{r_o - r_L}{c} \simeq \frac{L\cos\theta_o}{c} \quad . \tag{24}$$

This time delay is characteristic of the vertical diffraction across the effective length α^{-1} of the array projected onto the direction of observation. It can be seen from Eq. (22) that large values of the nondimensional parameter $\Gamma=r_o\cos\theta_o/L$ indicate a geometric farfield behavior. It is therefore a measure of the geometric nearfield of a stationary TA.

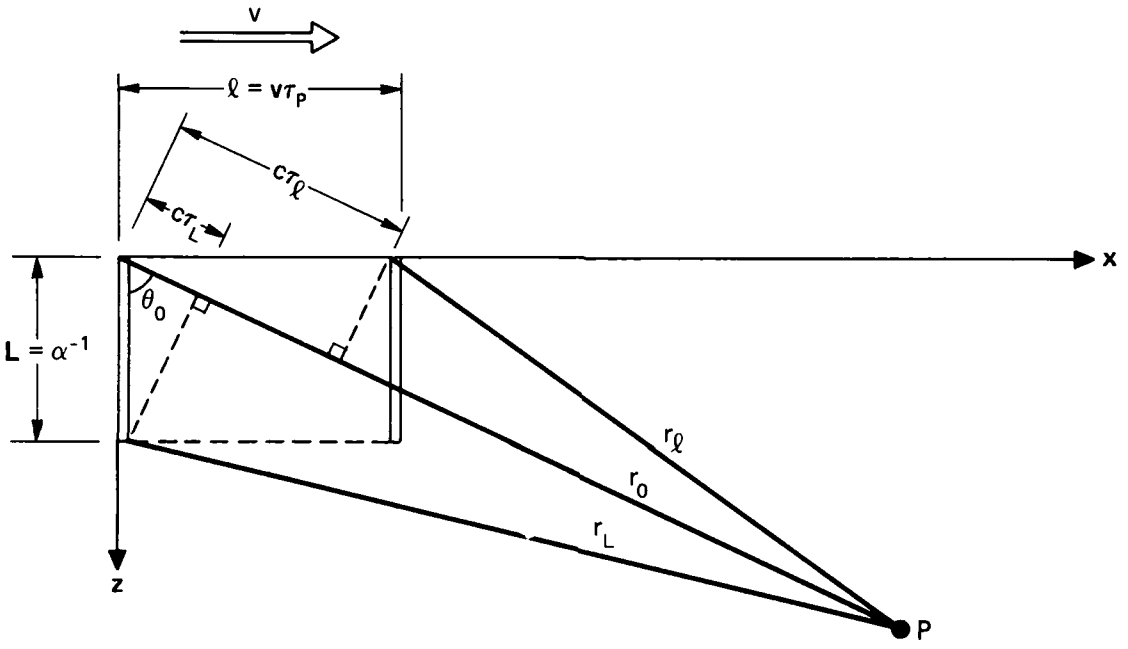

FIGURE 5
GEOMETRIC FARFIELD

ARL:UT
AS-84-783
YHB - GA
9 - 5 - 84

b. Moving Source

If the source is moving at velocity v in the +x direction during a time duration τ_p, it travels a distance $\ell = v\tau_p$. Now the source may be thought of as rectangular with dimensions $L \times \ell$. In order to be in the geometric farfield, both dimensions must be small relative to r_o. Hence ℓ will play a role similar to that of L in the previous discussion. The Fresnel approximation for the geometric farfield is then

$$\frac{\ell}{r_o} << 1 \quad , \tag{25}$$

or, if M=v/c,

$$\frac{r_o}{c\tau_p} >> M \quad . \tag{26}$$

Similarly we can define a time delay τ_ℓ characteristic of the horizontal diffraction due to the motion of the source (see Fig. 5),

$$\tau_\ell = \frac{r_o - r_\ell}{c} \quad , \tag{27}$$

where r_ℓ is the distance to the receiver from the array point at z=0 and $x=\ell$. For $\ell << r_o$, τ_ℓ reduces to

$$\tau_\ell \simeq \frac{\ell \sin\theta_o}{c} = M\tau_p \sin\theta_o \quad . \tag{28}$$

Equations (22) and (26) define the geometric farfield criterion. These equations are valid for both modulated and unmodulated source intensities.

2. Acoustic Farfield

The acoustic farfield criterion is a measure of the ratio of the distance of observation to a typical wavelength emitted by the source. The acoustic farfield approximation is therefore completely independent of the geometric farfield approximation.

a. Stationary Source

When the distance of observation r_o is much bigger than the wavelength λ emitted by the source, the observer is said to be in the (acoustic) farfield. This occurs when

$$kr_o >> 1 \quad , \tag{29}$$

where k is the wave number of the lowest frequency component present in the signal (most restrictive case).

For an unmodulated pulse, $k=2\pi/c\tau_p$, so the condition imposed by Eq. (29) becomes

$$\tau_p << \frac{r_o}{c} \quad . \tag{30}$$

For a monochromatic modulation of a signal at a frequency f_o (period T_o), $k=2\pi/cT_o$, so that the farfield condition can be expressed as

$$T_o << \frac{r_o}{c} \quad . \tag{31}$$

b. Moving Source

The previous section has just shown that the acoustic farfield is determined by the relative importance of the typical time scale of the pulse to the retarded time of observation r_o/c. However, when a source is in motion, it is well known that the time scale will change in accordance with the Doppler shift.[12] The acoustic farfield criterion can therefore be rewritten as

$$k_d r_o >> 1 \quad , \tag{32}$$

where k_d is the Doppler shifted wave number of the lowest frequency component in the signal. In the case of a point source moving at velocity v=Mc in the +x direction, k_d is related to k by

$$k_d = \frac{k}{|1-M \sin\theta_o|} \quad . \tag{33}$$

Using Eq. (33) as an approximation for the wave number of the thermoacoustic array, the acoustic farfield criterion for an unmodulated pulse of duration τ_p becomes

$$r_o >> c\tau_p \left|1-M \sin\theta_o\right| \quad . \tag{34}$$

For a pulse modulated every T_o seconds, the acoustic farfield occurs when

$$T_o \left|1-M \sin\theta_o\right| << \frac{r_o}{c} \quad . \tag{35}$$

Note that Eqs. (34) and (35) are always satisfied in the Čerenkov direction ($\sin\theta_o = M^{-1}$) so that for a source moving at velocity $c/\sin\theta_o$, the acoustic nearfield is virtually nonexistent. However, it must be borne in mind that Eqs. (34) and (35) are only crude approximations to the real physical problem--the Doppler shift introduced in these expressions is valid only for a point source. Moreover, the equations assume that the angle of observation remains constant during the motion of the source. This assumption is obviously violated at large Mach numbers. The exact Doppler shift of a thermoacoustic array moving at any velocity (including transonic) has been investigated in more detail[13] and will be presented in a separate report.

3. Source Dimensions

In Section IV, the results obtained with the impulse response technique described in Sections II and III will be compared with some results obtained in a previous study.[9] This comparison will be easier to make if we introduce the Fraunhofer approximation. It is important to

realize that this approximation is independent of the farfield approximations described previously. The Fraunhofer approximation depends only upon the dimensions of the source relative to the acoustic wavelength radiated by the source.

a. Stationary Source

Assume that the source is small in terms of an acoustic wavelength, i.e., that

$$kL << 1 \quad , \tag{36}$$

where L is the length of the source and k is the wave number of the highest frequency component in the signal (most restrictive case). This is the Fraunhofer approximation.[11]

• For an unmodulated pulse, $k=2\pi/c\tau_p$, so that by combining Eq. (24) and Eq. (36) we obtain

$$\tau_p >> \tau_L \quad . \tag{37}$$

• For an intensity modulated signal of period T_o, Eq. (36) can be rewritten as

$$T_o >> \tau_L \quad . \tag{38}$$

Equations (37) and (38) represent the small (stationary) source approximation for both unmodulated and modulated cases.

For a source that is large in terms of a wavelength (long narrow cylinder),

$$kL >> 1 \quad , \tag{39}$$

where k is the wave number of the lowest frequency component of the signal. For both modulated and unmodulated cases, $k=2\pi/c\tau_p$, and Eq. (39) can be rewritten as

$$\tau_p << \tau_L \quad . \tag{40}$$

b. Moving Source

Here again the time scale change (Doppler shift) will affect the characteristic wave number in Eq. (34) and Eq. (37) (refer to Section III.B.2.b). As in the case of the geometric farfield approximation, the motion of the source introduces a second dimension to the source. Therefore the source is small in terms of a wavelength if both the following equations are satisfied.

$$k_d L << 1 \tag{41}$$

and

$$k_d \ell << 1 \quad . \tag{42}$$

The small source approximation for an unmodulated pulse of duration τ_p becomes

$$\tau_{p,d} >> \tau_L, \tau_\ell \quad ; \tag{43}$$

and, for a modulated pulse of period T_o, becomes

$$T_{o,d} >> \tau_L, \quad \tau_\ell \quad , \tag{44}$$

where the subscript d indicates a Doppler shifted quantity. Similarly, if the source is long in terms of a wavelength,

$$\tau_{p,d} << \tau_L \quad , \tag{45}$$

and

$$\tau_{p,d} << \tau_{\ell} \quad . \tag{46}$$

Equation (45) indicates the characteristic of a long source in the z direction, while Eq. (46) indicates the property of a long source in the x direction. Both Eqs. (45) and (46) apply for either modulated or unmodulated laser pulse.

C. Results

In this section we present the results obtained using the impulse response technique to predict the pressure waveform radiated by a thermoacoustic array. We first discuss the laser pulse shape which has been chosen for the numerical predictions. We then restrict our attention to the results obtained when the source is stationary and the intensity unmodulated. Finally we show the theoretical predictions obtained in some realistic configurations of a moving and modulated laser pulse.

1. Laser Pulse

Muir et al.[5] have shown that a modulated laser intensity may be conveniently described by

$$I(t) = I_0(t) \sin^2\left(\frac{\omega t}{2}\right) = I_0(t) \left[1/2 - 1/2 \cos\omega t\right] \quad , \tag{47}$$

where $I_0(t)$ is the laser pulse envelope, and ω is the angular modulation frequency, that is, the acoustic frequency for a stationary source.

The laser pulse envelope $I_0(t)$ was determined from the actual laser used in the experimental study of thermoacoustic arrays at ARL:UT facilities. It was found that $I_0(t)$ is well represented by

$$I_0(t) = A\left(\frac{t}{\tau_p}\right) \exp\left(-B\,\frac{t}{\tau_p}\right) \quad , \tag{48}$$

with A=10.8 and B=5.0. The peak amplitude occurs at $t=\tau_p/B$, where τ_p is the laser pulse duration.

2. Stationary Unmodulated Laser Pulse

The impulse response approach described previously was used to predict the pressure waveform radiated by a stationary thermoacoustic array. The modulation frequency was set to zero in order to simplify the interpretation of the results. However, it should be understood that the computer program is not restricted to unmodulated pulses.

Figure 6 shows the evolution of the predicted pressure waveform received in fresh water at the observation point as the nondimensional parameter Γ changes from 200 to 0.2, i.e., from geometric farfield to nearfield values. The position of the receiving point is kept constant (r_o = 4 m and $\theta_o=60^o$) so that the variation of Γ corresponds in fact to the variation of the effective length ($L= \alpha^{-1}$) of the array, from 1 cm to 10 m (short array to long array). The pulse duration was set to 250 μsec so that the observation point was always located in the acoustic farfield ($kr_o=67$).

In the farfield case shown in Fig. 6(a), the pressure waveform is found to occur over a narrow time period and have a sharp peak at the onset, followed by a negative signal. The sharp peak in the acoustic response observed in Fig. 6(a) is due to the fact that the laser pulse described by Eq. (48) has a discontinuous time derivative at t=0. The inverted shape of the laser pulse which appears for all values of Γ in Figs. 6(a)-6(f) after the retarded time r_o/c can be explained by the effect of the pressure release interface between air and water. As will be shown in Section IV.A of this report, this farfield waveform is directly proportional to the second time derivative of the laser pulse intensity.

As shown in Figs. 6(b)-6(f), the pressure waveform broadens and changes substantially in shape as the situation approaches the geometric

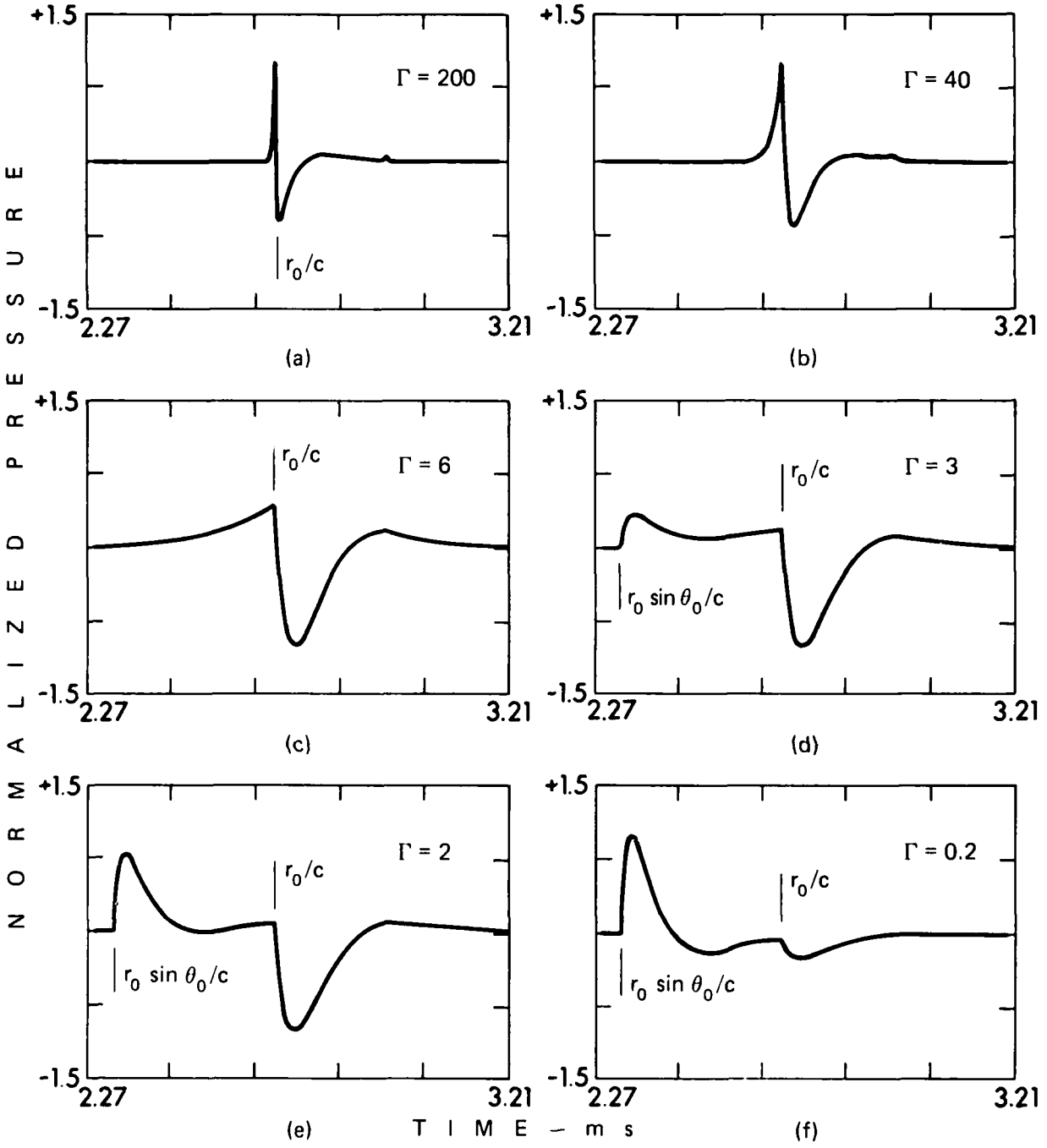

FIGURE 6
PRESSURE WAVEFORM AS A FUNCTION OF $\Gamma = \alpha r_0 \cos\theta_0$
FOR A STATIONARY UNMODULATED LASER PULSE
(r_0 = 4 m; $\theta_0 = 60^\circ$; τ_P = 250 μsec)

ARL:UT
AS-84-784
YHB - GA
9 - 5 - 84

nearfield. In the extreme nearfield represented by Fig. 6(f), the pressure waveform is seen to begin at time $t=r_0\sin\theta_0/c$ rather than the time $t=r_0/c$, at which the pressure signal begins in the farfield. This result agrees with the analysis presented in Section II.B. It is also interesting to note that in the extreme geometric nearfield of a very long and narrow TA (Fig. 6(f)), the acoustic response occurring at the retarded time r_0/c will be exactly an inverted laser pulse. This effect is also discussed in Section IV.B.

3. Moving Modulated Laser Pulse

Some typical pressure waveforms radiated by a moving thermoacoustic array are presented in Fig. 7. These waveforms were obtained by computer simulations, using the impulse response approach described previously. These predictions were made for realistic values of the important parameters: $r_0 = 4$ m, $\theta_0=75^0$, $\alpha = 15\ m^{-1}$, $f_0 = 7$ kHz, $\tau_p = 1$ msec, and $\Gamma=15.5$. The Mach number was varied from 0 to 1.5.

Table I, which shows the farfield measures as a function of the Mach number, indicates that the observation point was always in the acoustic farfield ($k_d r_0 >> 1$). However, it was in the geometric nearfield for M=1.04 and M=1.5. Table I also shows that the source used in generating Fig. 7 was always long in both the x and z directions in terms of a wavelength, except when the source was stationary.

Figure 7(a) shows the acoustic responses of a modulated, stationary thermoacoustic array. There is a periodic nature to the response with a roughly exponential decay in the amplitude corresponding to the exponential decay in the laser intensity (see Eq. (48)).

Figures 7(b), 7(c), and 7(d) show the acoustic response of a moving modulated thermoacoustic array. Note that these figures show waveforms of different shapes than the stationary array. Some of the changes caused by the motion of the array are the result of moving into the geometric

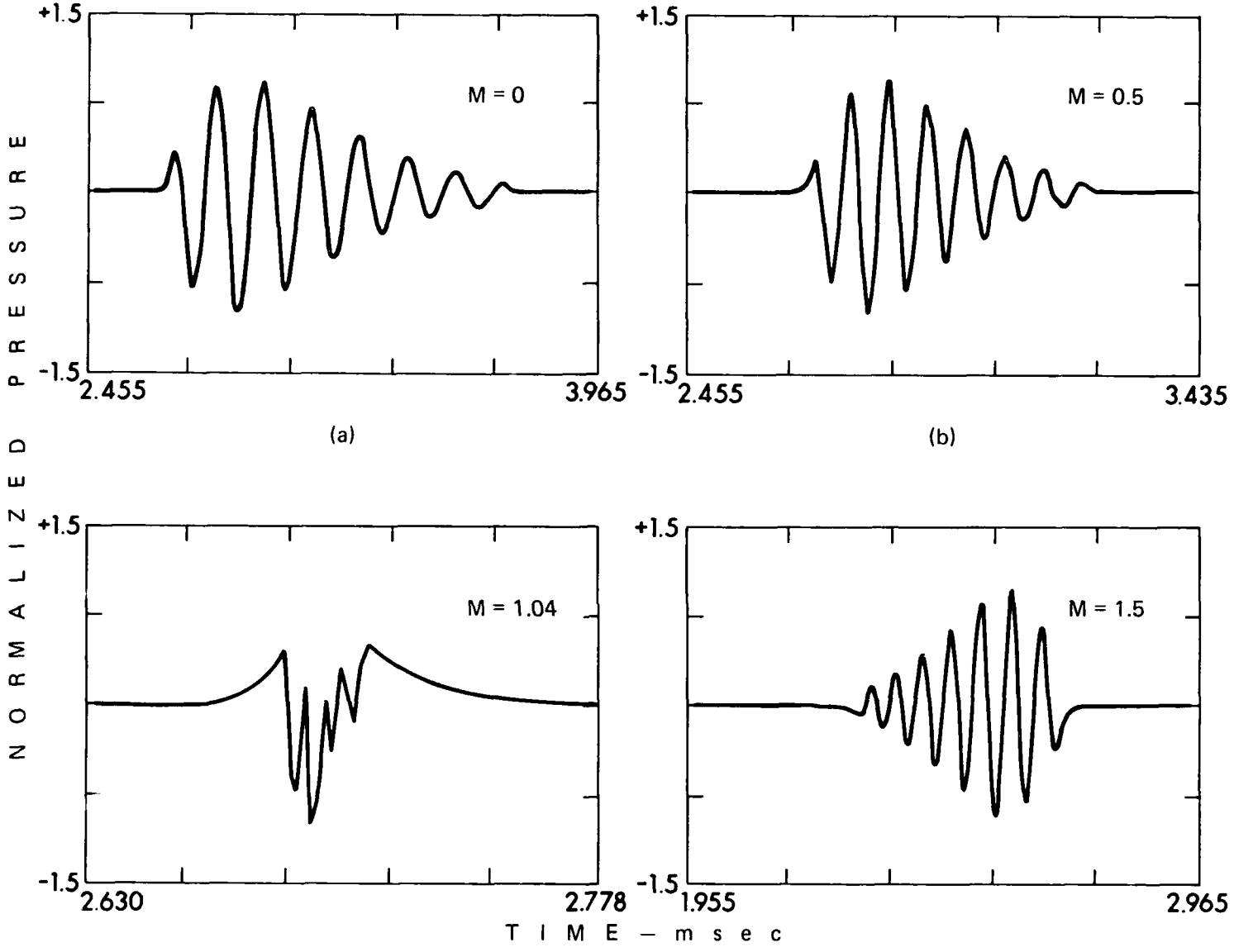

ARL:UT
AS84-785
YHB:GA
9-5-84

FIGURE 7
ACOUSTIC RESPONSE OF A MOVING THERMOACOUSTIC ARRAY

TABLE I

FARFIELD LIMIT FOR THE THERMOACOUSTIC WAVES PLOTTED IN FIGURE 7

Figure	Mach	Geometric Farfield		Acoustic Farfield		Source Dimensions Farfield Criterion	
		r_o/L	r_o/ℓ	$k_d r_o$	$k_d L$	$k_d \ell$	$k_d L$
7(a)	0	60	∞	11.84	2.0	0	2.0
7(b)	0.5	60	5.4	228.9	3.8	42.4	3.8
7(c)	1.04	60	2.6	∞	∞	∞	∞
7(d)	1.5	60	1.8	263.6	4.4	146.4	4.4

nearfield. Other changes are caused by the time compression which occurs for nonstationary sources.

One advantage of the time domain approach, used in the numerical computation of the pressure waveform, is that the Doppler shift is implicitly taken into account by the time delays of the pseudo-convolution. Therefore the Doppler shift appears naturally and is valid not only for a point source, but also for an extended array of length α^{-1}. This is discussed thoroughly by Berthelot and Busch-Vishniac,[13] who show that the effect of having an extended source instead of a point source is to reduce the pressure amplitude measured in the Čerenkov direction. This is why the computed pressure waveform is always bounded even for a Mach wave (see Fig. 7(c)).

The case of a thermoacoustic array moving at transonic velocity deserves special attention because it yields the maximum peak power of the optoacoustic source. A detailed analysis of the Doppler shift associated with a transonic source may be found in Ref. 13. The difficulty arising with transonic source motion is the assumption that the laser beam diameter is small compared to an acoustic wavelength. This assumption is clearly violated at transonic velocities because in that case the Doppler shifted acoustic wavelength goes to zero. It is therefore essential to include the effects of the finite width of the laser beam on the pressure waveform radiated by a transonic thermoacoustic array. A report describing these finite effects is being prepared.

In order to analyze Figs. 7(b) and 7(d), we may, however, simplify the problem and use as a first approximation the classical Doppler factor formulation[12] without any finite beamwidth effects. In the formulation, the Doppler factor D is given by

$$D = \left| 1 - \frac{v}{c} \sin \theta_o \right| \quad . \tag{49}$$

Equation (49) indicates that a modulation frequency f_o of 7 kHz should give a Doppler shifted frequency $f_d = f_o/D$ of about 13.5 kHz at M=0.5 and

13. Y. H. Berthelot and I. J. Busch-Vishniac, "Radiation from an Acoustic Array Moving at Transonic Velocities," J. Acoust. Soc. Am. 75, 523 (1984), and "The Doppler Shift of an Acoustic Source Moving at Transonic Velocities," submitted for publication, J. Acoust. Soc. Am.

14. J. W. S. Rayleigh, The Theory of Sound, 2nd Edition (Dover Publications, New York, 1945), Vol. II, Art. 298, p. 154.

15. P. M. Morse and K. U. Ingard, Theoretical Acoustics (McGraw-Hill Book Co., Inc., 1968), Chpt. 12, p. 783.

16. P. J. Westervelt, "Parametric End-Fire Array," J. Acoust. Soc. Am. 32(A), 934-935 (1960). Also see "Parametric Acoustic Array," J. Acoust. Soc. Am. 35, 535-537 (1963).

17. B. K. Novikov, D. V. Rudenko, and V. I. Timoshenko, Nonlinear Hydroacoustic (Sudostroyeniye, Leningrad, 1981), Chpts. 2, 5, and 9. (In Russian)

18. Hsiao-an Hsieh and Allan D. Pierce, "Some Possible Novel Configurations for Optico-Acoustic Transducer Arrays Created by Controlled Motion of Laser Beams across Water Surfaces," J. Acoust. Soc. Am. 75, S16 (1984).

REFERENCES

1. A. G. Bell, "Upon the Production of Sound by Radiant Energy," Philoso. Mag. (Ser. 5) 11, 510 (1881).

2. P. J. Westervelt and R. S. Larson, "Laser-Excited Broadside Array," J. Acoust. Soc. Am. 54, 121-122 (1973).

3. R. S. Larson, "Optoacoustic Interactions in Fluids" (U), Applied Research Laboratories Technical Report No. 74-21 (ARL-TR-74-21), Applied Research Laboratories, The University of Texas at Austin, May 1974.

4. T. G. Muir: "Experiments on Laser-Excited Array," J. Acoust. Soc. Am. 54, 298(A) (1973).

5. T. G. Muir, C. R. Culbertson, and J. R. Clynch, "Experiments on Thermoacoustic Arrays with Laser Excitation," J. Acoust. Soc. Am. 59, 735-743 (1976).

6. C. R. Culbertson, "Experimental Investigation of the Laser-Excited Thermoacoustic Array in Water," Masters Thesis, The University of Texas at Austin (1975); also, Applied Research Laboratories Technical Report No. 75-51 (ARL-TR-75-51), Applied Research Laboratories, The University of Texas at Austin.

7. F. V. Bunkin et al., "Experimental Investigation of the Acoustic Field of a Moving Optoacoustic Antenna," Sov. J. Quantum Electron. 8(2), 270-271 (1978).

8. F. V. Bunkin et al., "Experimental Study of Pulsed Sound Fields Excited by Moving Laser Thermooptical Sources," Sov. Phys.-Acoust. 27(2), 98-102 (1981).

9. L. M. Lyamshev and L. V. Sedov, "Optical Generation of Sound in a Liquid: Thermal Mechanism (Review)," Sov. Phys.-Acoust. 27(1), 4-18 (1981).

10. M. Abramowitz and I. A. Stegun, Handbook of Mathematical Functions, 9th Edition (Dover Publications, Inc., New York, 1970).

11. J. W. Goodman, Introduction to Fourier Optics (McGraw-Hill Book Company, Inc., New York, 1968), Chpt. 5.

12. A. D. Pierce, Acoustics: An Introduction to Its Physical Principles and Applications (McGraw-Hill Book Company, Inc., 1981), Sec. 9.3.

It is also convenient to relate the energy q, added to the medium, to the intensity of the laser beam illuminating the medium. Let us denote by $\langle \vec{I} \rangle$ the intensity of the laser beam averaged over a period of the (very rapid) optical oscillation of the laser light. $\langle \vec{I} \rangle$ is called the Poynting vector of the process. Then the flux of intensity $\nabla \cdot \langle \vec{I} \rangle$ represents just the heat absorbed by the medium (per unit time and unit volume). Therefore it follows from the definition of q that

$$q = - \nabla \cdot \langle \vec{I} \rangle \quad . \tag{A.17}$$

In practice the laser beam is shining in, say, the +z direction, so that $q = - \frac{\partial I}{\partial z}$.

Equations (A.16) and (A.17) are the starting point of the theory presented in this report.

It is interesting to note that Eq. (A.16) has exactly the same form as *the Westervelt inhomogeneous wave equation*[16] *describing parametric end-fire* radiation. In the wave equation for the parametric array, however, the source term represents virtual sources generated by nonlinear interaction in the medium, whereas in Eq. (A.16) the source term represents the time and spatial derivative of the intensity distribution in the laser beam. There is nevertheless a close mathematical analogy between parametric arrays and thermoacoustic arrays, and this analogy has been used by Novikov, Rudenko, and Timoshenko[17] to study the pressure waveform radiated by a transonic thermoacoustic array.

$$\rho = c^{-2}p - s\rho_o \beta T_o c_p^{-1} \quad , \tag{A.10}$$

and the last term in Eq. (A.10) represents the effect of the laser heating on the change of density in the medium. Since we seek a wave equation for the acoustic pressure p, we eliminate $\vec{u}$ between Eq. (A.1) and (A.2). It is found that

$$\nabla^2 p - \rho_{tt} + \left(\frac{\lambda + 2\mu}{\rho_o}\right)\nabla^2 \rho_t = 0 \quad . \tag{A.11}$$

Eliminating the ρ between Eq. (A.10) and Eq. (A.11) yields a wave equation for the acoustic pressure p and the input entropy s,

$$\nabla^2 p - \left[c^{-2}p_{tt} - s_{tt}\, \rho_o\, \beta T_o c_p^{-1}\right] + \left(\frac{\lambda+2\mu}{\rho_o}\right) \nabla^2 \left[c^{-2}p_t - s_t\, \rho_o\, \beta T_o c_p^{-1}\right] = 0 . \tag{A.12}$$

Now let us relate the change in entropy s to the heat q added to the medium by the laser beam. The conservation law which governs that relation is the second law of thermodynamics for a reversible process,

$$\bar{\rho}\, \bar{T}\, ds = q\, dt \tag{A.13}$$

or, in linearized form,

$$\rho_o T_o s_t = q \quad . \tag{A.14}$$

Combining Eq. (A.14) with Eq. (A.12) to eliminate the entropy fluctuation s yields

$$\nabla^2 p - \frac{1}{c^2} p_{tt} + \left(\frac{\lambda + 2\mu}{\rho_o c^2}\right) \nabla^2 p_t = - \frac{\beta}{c_p} q_t + \left(\frac{\lambda + 2\mu}{\rho_o}\right) \left(\frac{\beta}{c_p}\right) \nabla^2 q . \tag{A.15}$$

This is the Westervelt-Larson equation for a viscous (but not heat conducting) irrotational medium containing a heat source of strength q. For a lossless medium, it reduces to the classical form

$$\nabla^2 p - \frac{1}{c^2} p_{tt} = - \frac{\beta}{c_p} q_t \quad . \tag{A.16}$$

Forming a Taylor series expansion of Eq. (A.3) about the equilibrium quantities ρ_o, p_o, and s_o, we have

$$\bar{\rho} = \rho_o + \left(\frac{\partial\bar{\rho}}{\partial\bar{p}}\right)_s (\bar{p}-p_o) + \left(\frac{\partial\bar{\rho}}{\partial\bar{s}}\right)_p (\bar{s}-s_o) + \ldots . \qquad (A.4)$$

By definition the small signal sound speed is $c = \left[\left(\frac{\partial p}{\partial\rho}\right)\right]_s^{1/2}$, so that Eq. (A.4) can be rewritten as

$$\rho = c^{-2}p + s\left(\frac{\partial\bar{\rho}}{\partial\bar{s}}\right)_p . \qquad (A.5)$$

The partial derivative in Eq. (A.5) is the result of the change in density due to the change in entropy induced by the laser heating. It is therefore related to the coefficient of thermal expansion β of the medium.

By definition

$$\beta = -\frac{1}{\bar{\rho}}\left(\frac{\partial\bar{\rho}}{\partial\bar{T}}\right)_p \qquad (A.6)$$

or

$$\beta = -\frac{1}{\bar{\rho}}\left(\frac{\partial\bar{\rho}}{\partial\bar{s}}\right)_p \left(\frac{\partial\bar{s}}{\partial\bar{T}}\right)_p . \qquad (A.7)$$

But it is well known from thermodynamics that the specific heat at constant pressure c_p can be expressed as

$$c_p = \bar{T}\left(\frac{\partial\bar{s}}{\partial\bar{T}}\right)_p . \qquad (A.8)$$

Combining Eq. (A.8) with (A.7), and linearizing the result about the undisturbed values, yields

$$\left(\frac{\partial\bar{\rho}}{\partial\bar{s}}\right)_p = -\rho_o \beta T_o c_p^{-1} ; \qquad (A.9)$$

therefore, Eq. (A.5) becomes

The wave equation describing the pressure field of a lossless medium containing a heat source can be found in Ref. 15. Starting from this thermoacoustic wave equation, Westervelt and Larson studied[2] the special case of a laser-induced sound field, discovering then the fascinating properties of what is now called a thermoacoustic array. In this appendix we rederive from the hydrodynamical equations of motion the Westervelt-Larson wave equation for laser-induced sound, including now the effect of viscosity.

Let $\bar{p}=p_0+p$ be the total pressure in the medium, where p_0 is the ambient pressure and p is the acoustic pressure generated through the thermal mechanism. Similarly let $\bar{\rho} = \rho_0+\rho$ be the total density of the medium, $\bar{T}=T_0+T$ be the total temperature, and $\bar{s}=s_0+s$ be the total entropy. The subscript o refers to an undisturbed quantity.

Since the acoustic disturbances generated by the thermal mechanism are expected to be small, we start directly from the linearized hydrodynamical equations of motion: the conservation of mass and the conservation of linear momentum.

$$\text{mass:} \quad \rho_t + \rho_0 \vec{\nabla} \cdot \vec{u} = 0 \tag{A.1}$$

$$\text{momentum:} \quad \rho_0 \vec{u}_t + \vec{\nabla} p = (\lambda + 2\mu) \nabla^2 \vec{u} \quad . \tag{A.2}$$

Here $\vec{u}$ denotes the particle velocity, $(\lambda+2\mu)$ represent the viscosity of the medium, and the subscript t denotes a time derivative.

It is implicitly assumed in Eqs. (A.1) and (A.2) that the medium is at rest, steady, uniform, and irrotational, and that heat conduction can be neglected.

The thermal input from the laser intensity induces a change in entropy in the system, so that an equation of state describing the process is

$$\text{state:} \quad \bar{\rho} = \bar{\rho}(\bar{p},\bar{s}) \tag{A.3}$$

APPENDIX A

THE INHOMOGENEOUS VISCOUS WAVE EQUATION FOR LASER-INDUCED SOUND

(2) Extension of the theory to include the effect of the finite beamwidth of the laser, with a Gaussian intensity distribution across a horizontal section of the beam.

(3) Generation of theoretical directivity patterns in the horizontal and vertical planes.

Experimental work on moving thermoacoustic arrays is also in progress and will be presented in a later report.

V. CONCLUSIONS

A time domain approach has been developed for the numerical computation of the pressure waveform radiated by a moving thermoacoustic array. The numerical results obtained are in good agreement with analytical expressions obtained from a frequency domain approach,[9] valid only in the farfield, and for either very short or very long arrays. The major advantages of the model described in this report are listed below.

(1) The model is valid in the nearfield of the source.

(2) It is not restricted to the limiting cases of very short or very long arrays.

(3) It does not require transforms to get time information.

(4) It is valid for a source moving at any velocities including the transonic case, and it can also be extended to the case of nonuniform source velocities.

(5) It is not restricted in principle to the case of a source moving rectilinearly, and it seems particularly appropriate in describing the promising case of a source moving along any discontinuous or curved paths.[18]

Further work on the theory presented here can be divided into three tasks.

(1) Extension of the theoretical model to the general case where the observation point is not necessarily in the plane of motion of the source.

The total pressure waveform received in the farfield can therefore be expressed as

$$p_T(t) \propto \delta'\left(t - \frac{r_o}{c}\right) * I'(t) = I''\left(t - \frac{r_o}{c}\right) \quad . \tag{50}$$

B. Long Array

The case of a long and narrow thermoacoustic array has also been treated by Lyamshev and Sedov[9] for farfield radiation. They found that the pressure waveform can be written* in the form

$$p = -K_{LS}\left\{ I\left(t - \frac{r_o}{c}\right) - \frac{\pi \tilde{q}}{\tau_\mu} \exp\left[-\left|\frac{t - \frac{r_o}{c}}{\tau_\mu}\right|\right]\right\} \quad , \tag{51}$$

where $\tilde{q} = \int_0^{\tau_p} I(t)dt$ is the "area" of the laser pulse and K_{LS} is a constant of proportionality containing the spherical spreading term r_o^{-1}, and $\tau_\mu = \cos\theta_o/\alpha c$. It turns out that the exponential term in Eq. (51) is of negligible order, and keeping this term is inconsistent with some other approximations assumed in their derivation. Therefore, the pressure waveform can be written simply as

$$p = -K_{LS}\, I\left(t - \frac{r_o}{c}\right) \quad . \tag{52}$$

Equation (52) describes an inverted laser pulse. As indicated in Fig. 8(b), the convolution approach described in this report reduces almost perfectly to Eq. (52) when the source has the shape of a long and narrow cylinder and for a receiver located in the farfield.

*A typographical error appears in Eq. (13), Ref. 9, p. 11. In Lyamshev and Sedov's notation, the exponent of the exponential should be divided by τ_μ.

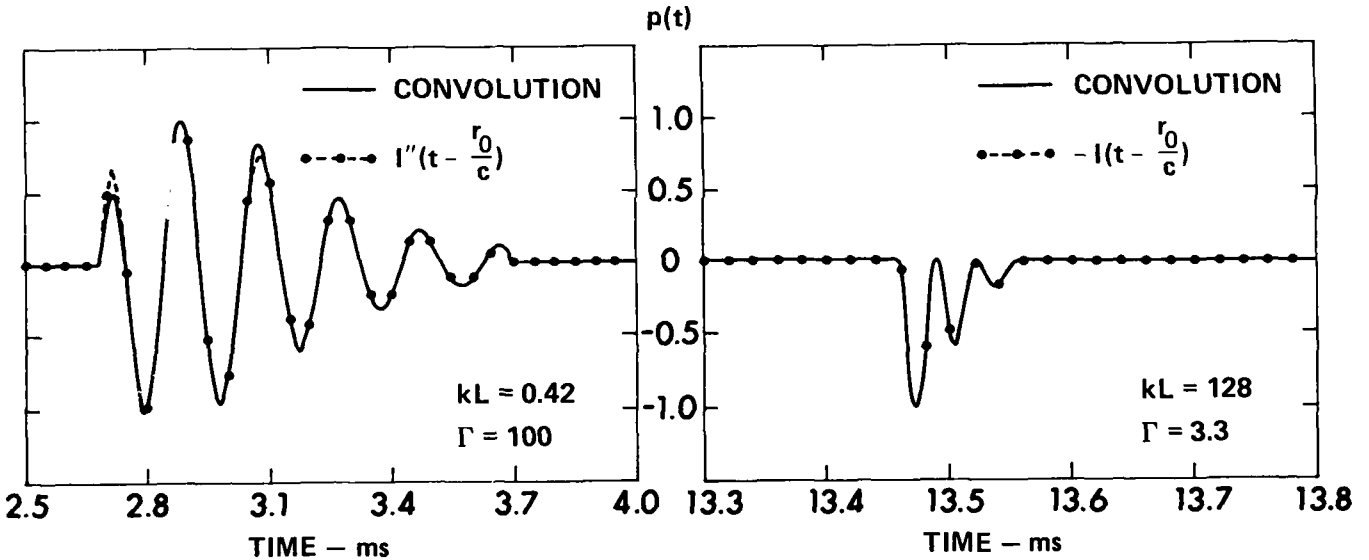

r_0 = 4 m $\quad \theta_0$ = 60°

f_0 = 5 kHz $\quad \alpha$ = 50 m^{-1}

r_0 = 20 m $\quad \theta_0$ = 60°

f_0 = 30 kHz $\quad \alpha$ = 0.33 m^{-1}

FIGURE 8
FARFIELD COMPARISON
(STATIONARY SOURCE)

ARL:UT
AS-83-1132-S
YHB-GA
10-24-83

IV. COMPARISON WITH PREVIOUS WORK

The numerical results obtained by the impulse response approach described in the previous sections can be compared with some analytical expressions obtained by Lyamshev and Sedov[9] for the special case of farfield radiation.

A. Short Array

It is shown in Ref. 9 that, in the acoustic farfield, the pressure waveform radiated by a thermoacoustic array is proportional* to the second time derivative of the laser pulse intensity, provided the effective length ($L = \alpha^{-1}$) of the array is very small compared to a typical acoustic wavelength.

Figure 8(a) shows that, under these assumptions, both the numerical and the analytical methods are in excellent agreement. The comparison was made for a modulation frequency of 5 kHz, a laser pulse duration of 1 msec, and for a stationary array. In this case the numerical program performs exactly a convolution.

The reason one should expect a pressure response proportional to the second derivative of the laser intensity can be explained in the time domain with the impulse response approach. When the thermoacoustic array is stationary, the pressure response $p_T(t)$ can be expressed as a convolution between the impulse response $h(t)$ and the time derivative of the laser intensity. However, in the geometric farfield ($L \ll r_o$) of a short array ($kL \ll 1$), the impulse response tends to behave like the time derivative of a delta function centered at time $t=r_o/c$. This is clearly shown in Fig. 4. The physical explanation for this behavior lies in the pressure release characteristics of the boundary between air and water.

*The "minus" sign, on the right-hand side of Eq. (12) in Ref. 9, should be read as a plus sign.

f_d = 15.6 kHz at M=1.5. This is in reasonable agreement with the Doppler shifted frequencies of 13.6 kHz and 16.0 kHz in Figs. 7(b) and 7(d).

Finally, it is interesting to note in Fig. 7(d) that time inversion effectively occurs at supersonic source velocities. This is due to the fact that, for a source moving faster than the acoustic disturbances it generates, the first signal to arrive at the receiving point will be the last one emitted by the source, provided the source is moving towards the receiver. This time inversion or phase reversal has been known for more than a century.[14]

4 December 1984

DISTRIBUTION LIST FOR
ARL-TR-84-21
UNDER CONTRACT N00014-82-K-0425

Copy No.

Office of Naval Research
Department of the Navy
Arlington, VA 22217
1 Attn: R. Fitzgerald

Director
Naval Research Laboratory
455 Overlook Ave., S.W.
Washington, DC 20375
2 Attn: Code 2627

3 - 14 Commanding Officer and Director
Defense Technical Information Center
Bldg. 5, Cameron Station
Alexandria, VA 22314

Naval Surface Weapons Center
White Oak Laboratory
Silver Spring, MD 20910
15 Attn: C. Bell

School of Mechanical Engineering
Georgia Institute of Technology
Atlanta, GA 30332
16 Attn: A. Pierce
17 P. Rogers

Mechanical Engineering Department
The University of Texas at Austin
Austin, TX 78712
18 Attn: I. Busch-Vishniac
19 D. Wilson

Electrical Engineering Department
The University of Texas at Austin
Austin, TX 78712
20 Attn: M. Becker

21 Advanced Sonar Division, ARL:UT

22 Yves H. Berthelot, ARL:UT

Distribution List for ARL-TR-84-21 under Contract N00014-82-K-0425 (cont'd)

Copy No.	
23	David T. Blackstock, ARL:UT
24	Nicholas P. Chotiros, ARL:UT
25	Reuben H. Wallace, ARL:UT
26	Library, ARL:UT
27 - 37	Reserve, ARL:UT

END

FILMED

8-85

DTIC